



# A synoptic characterization of the dust transport and associated thermal anomalies in the Mediterranean basin

Marco Gaetani (1,2), Massimiliano Pasqui (2),  
Alfonso Crisci (2), Francesca Guarnieri (2,3)

(1) Dep Geofísica y Meteorología,  
Universidad Complutense de Madrid, Espana

(2) IBIMET-CNR, Roma & Firenze, Italia

(3) Consorzio LAMMA, Sesto Fiorentino, Italia

XXXII Jornadas Científicas de la AME  
"Meteorología y Calidad del Aire"  
Museo de la Ciencia COSMOCAIXA MADRID  
28-30 de Mayo de 2012

*Puerta del Sol,  
Madrid,  
12 Mayo 2012*

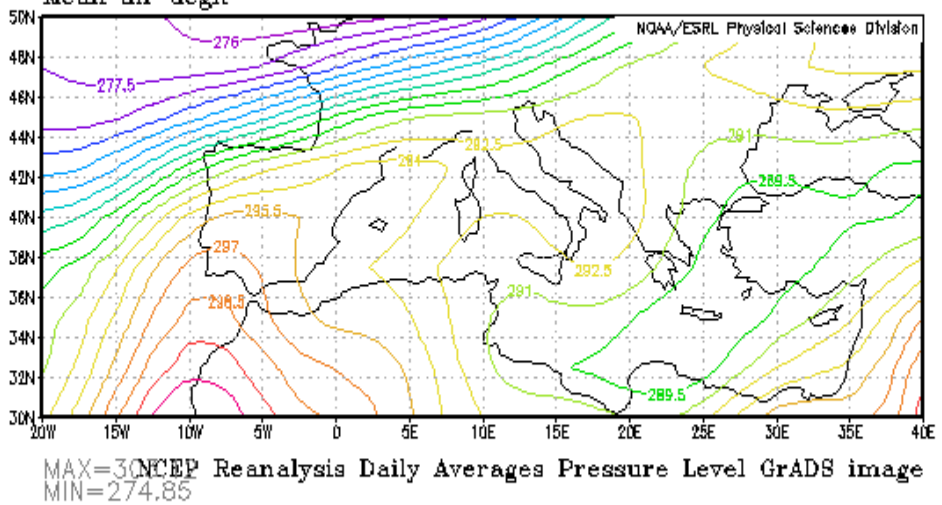
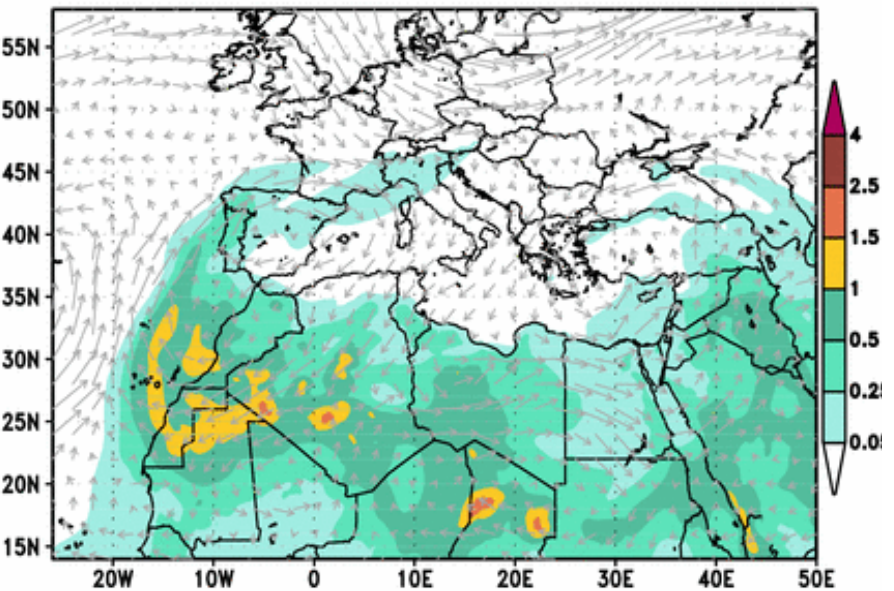


*Barcelona Supercomputing Center - DREAM8b Forecast*

*NCEP Reanalysis*

BSC-DREAM8b Dust Loading (g/m<sup>2</sup>) and 3000m Wind  
0h forecast for 12UTC 12 MAY 12

lon: plotted from -20 to 40.00  
lat: plotted from 30.00 to 50.00  
lev: 925.00  
t: May 12 2012  
Mean air degK



MAX=30.00 NCEP Reanalysis Daily Averages Pressure Level GrADS image  
MIN=274.85

## Natural mineral aerosol (dust) interaction with climate

Direct influence > affects atmospheric radiative balance through the modification of the optical thickness > consequences on the heat content (Tegen et al., 1997; Alpert et al., 1998).

Indirect influence > induces changes in the clouds microphysical dynamics > consequences on precipitation and albedo (Rosenfeld et al., 2001; Mahowald, Kiehl, 2003).

## Impact of Saharan dust on the Mediterranean atmosphere

Radiative forcing > decrease of daily mean solar radiation reaching the surface > reduction of the planetary boundary layer height and the horizontal wind speed (Péré et al., 2011).

Interaction with clouds and precipitation > production of giant CCN > increased precipitation rates (Levin et al., 1996; Wurzler et al., 2000; Levin et al., 2005).

## Impact on human health

- > Influence on the concentration and transport of **pollutants** (Bonasoni et al., 2004; Bergametti et al., 1989; Erel et al., 2006) .
- > Contribution to the **particulate matter (PM) concentration across the Mediterranean countries** (Querol et al., 2009) > a substantial number of exceedances of the PM10 daily limit value (50  $\mu\text{g}/\text{m}^3$ , EU/2008/50 European Union directive) has been attributed to Saharan dust outbreaks (Koçak et al., 2007; Pederzoli et al., 2010) .
- > **Iberian peninsula: the majority of the PM10 (70% in most stations) and PM2.5 (17–55% in most stations) exceedances in regional background monitoring stations are caused by African dust outbreaks (Escudero et al., 2007) .**

# Saharan dust transport over the Mediterranean

Prominent between March and September, with maxima in spring in the East Med and in summer in the West Med;

Spring transport > transit of the Sharav cyclones over North Africa;

Summer transport > coupling between the Balearic low and the Saharan high.

MOULIN ET AL.: SATELLITE CLIMATOLOGY OF AFRICAN DUST TRANSPORT

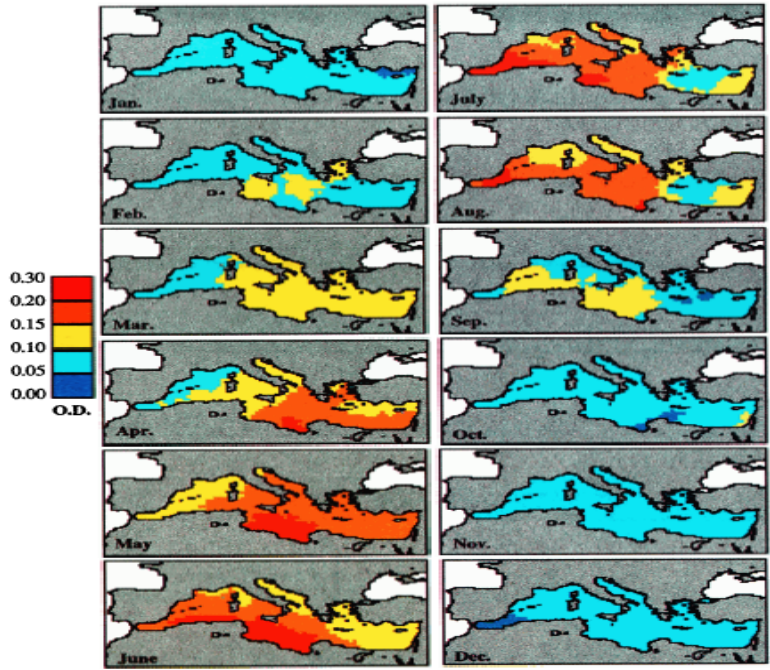


Plate 1. Monthly 11-year average of dust optical depths (O.D.). Data from available Meteosat images between 1984 and 1994 (see Table 1).

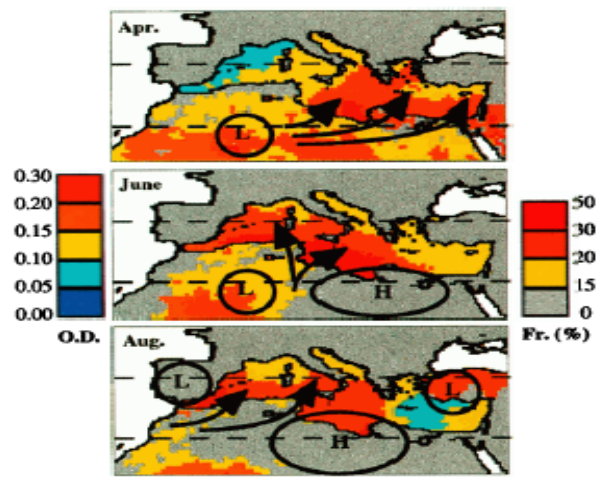


Plate 2. How the main meteorological synoptic situations generate a recurrent dust transport during spring and summer. Locations of the major lows (L) and highs (H) are shown. The cyclogenesis is adapted from Alpert et al. [1990]. It shows the Sharav cyclones in April; the coupling between Saharan low and Libyan high in June; and the effect of the Balearic cyclogenesis in August. The frequency (Fr.) of dust mobilization over North Africa during these months has been estimated from IDDI computed from Meteosat infrared images between 1984 and 1994, using the method of Legrand et al. [1994]. Finally, our monthly dust optical depths (O.D.) over the sea surface are shown as in Plate 1. The lower and upper horizontal dashed lines correspond to latitudes of 30° and 40°N, respectively.

Moulin et al, 1998 JGR

## Objective

> Characterization of the daily dust transport in the Mediterranean region, through the association with circulation patterns identified using Circulation Types Classification (CTC) methods based on Principal Components Analysis (PCA).

### Daily AOD at 550 nm:

- GOCART model (Chin et al., 2002),  $2^{\circ} \times 2.5^{\circ}$  lat-lon, 2000-2007;
- MODIS (King et al., 2003)  $1^{\circ}$  horizontal resolution, 2001-2010.

### Daily atmospheric fields:

NASA MERRA dataset (Rienecker et al., 2011),  $1.25^{\circ}$  horizontal resolution, 1979-2010.

## Circulation Types Classification

Circulation patterns derived from two CTC methods based on PCA:

- PCT (obliquely rotated PCA of subsamples in T-mode)
- PXE (Pca-eXtreme scores reassigned by Euclidean distance) (Philipp et al., 2010).

Evaluation metric:

- Explained Variation =  $1 - \text{WSS} / \text{TSS}$

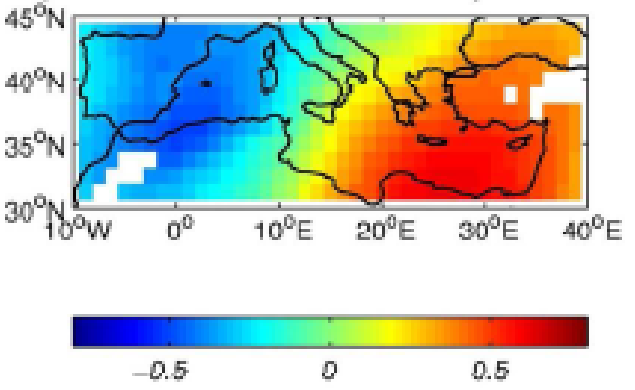
The methods are implemented in the framework of the European Cooperation in Science and Technology (COST) Action 733 "Harmonisation and Applications of Weather Types Classifications for European Regions" (<http://cost733.met.no>), the CTCs are computed using the `cost733class-1.0 software` (Philipp et al., 2010; Demuzere et al., 2011).

# SVD AOD vs T850

Connection with thermal advectons and intra-basin varability > T850 and AOD indices

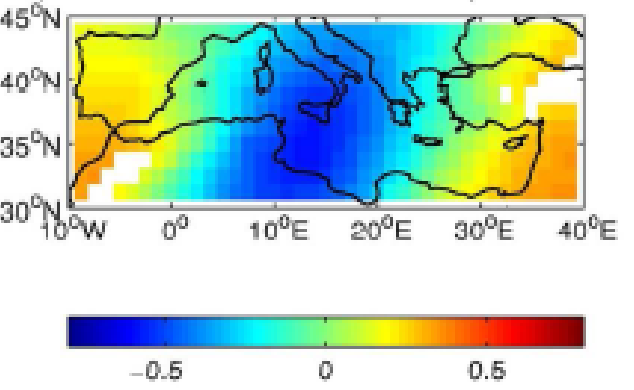
T850-1  
EM / WM

a) MERRA T850: cov-mode 1 | SCF=0.60



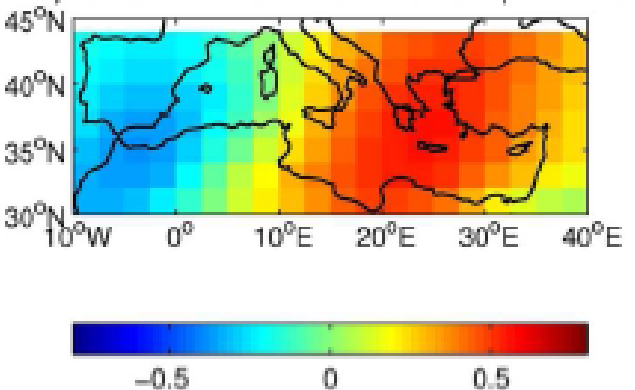
T850-2  
CM

b) MERRA T850: cov-mode 2 | SCF=0.31



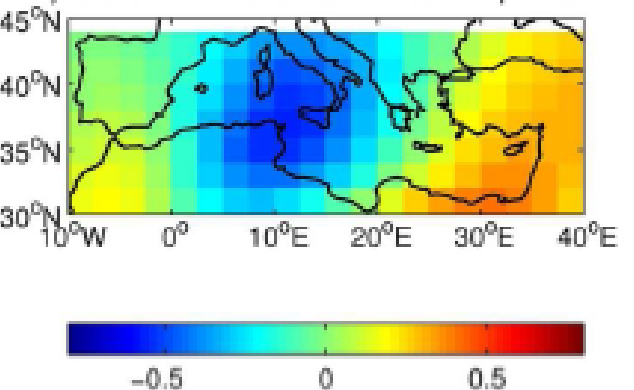
AOD-1  
EM / WM

c) GOCART AOD: cov-mode 1 | R=0.70



AOD-2  
CM

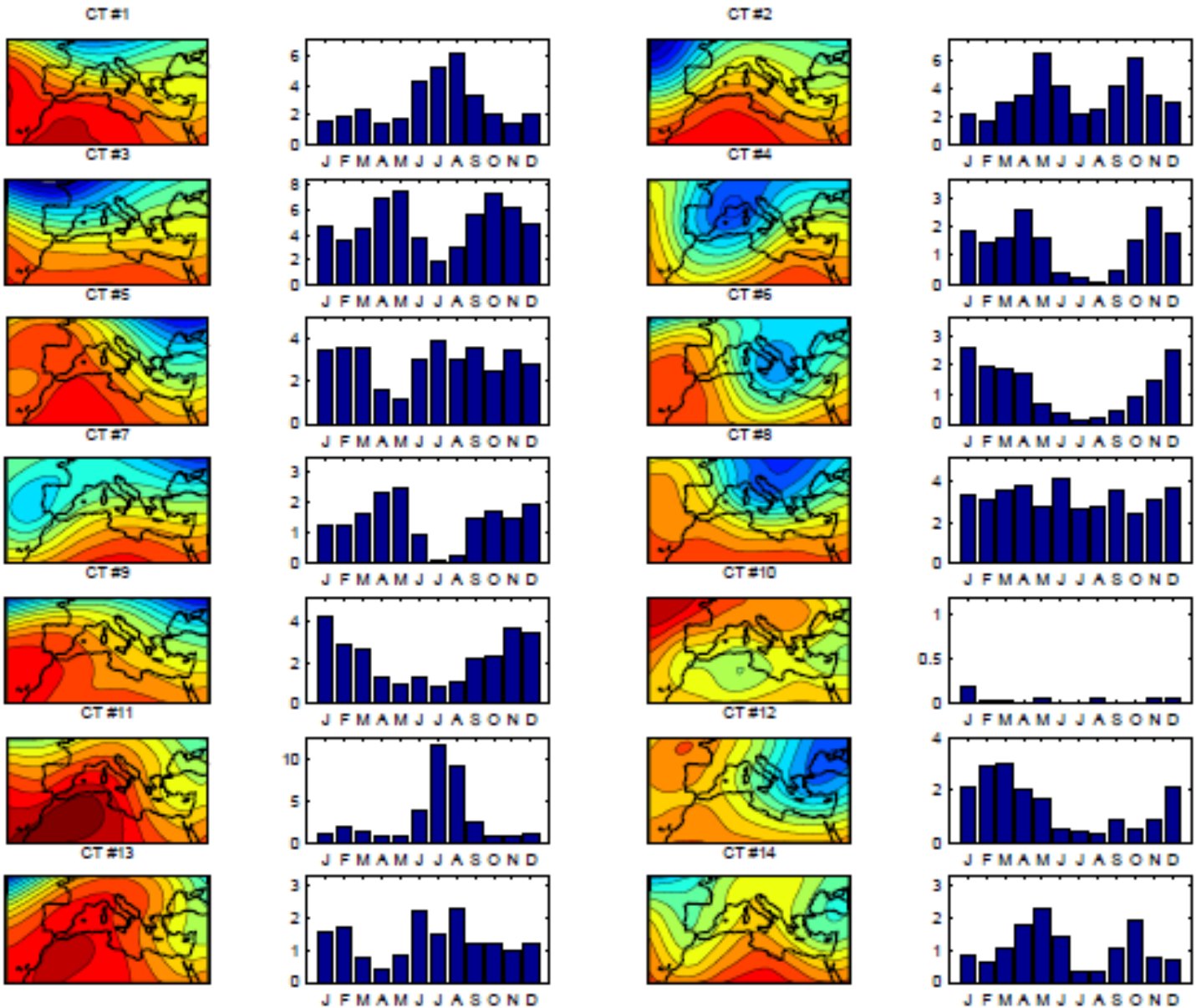
d) GOCART AOD: cov-mode 2 | R=0.64



2000-2007 MCA applied to MERRA T850 and GOCART AOD daily anomalies, 1st (left panels) and 2nd (right panels) covariance mode displayed through heterogeneous correlation maps of T850 (a,b) and AOD (c,d).



# PCT 14, centroids and frequencies (characterization of the WM and EM variability)

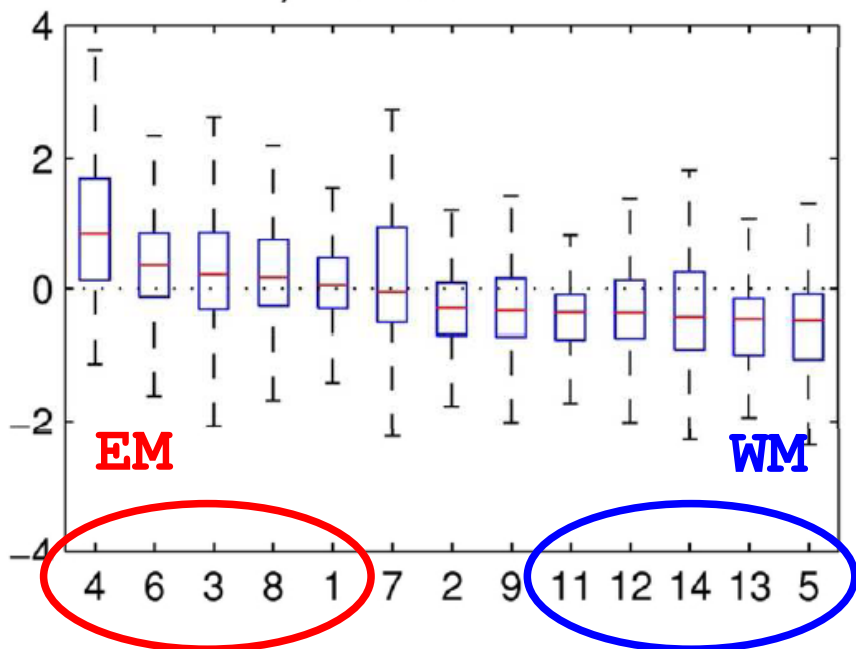


## Circulation-to-environment approach

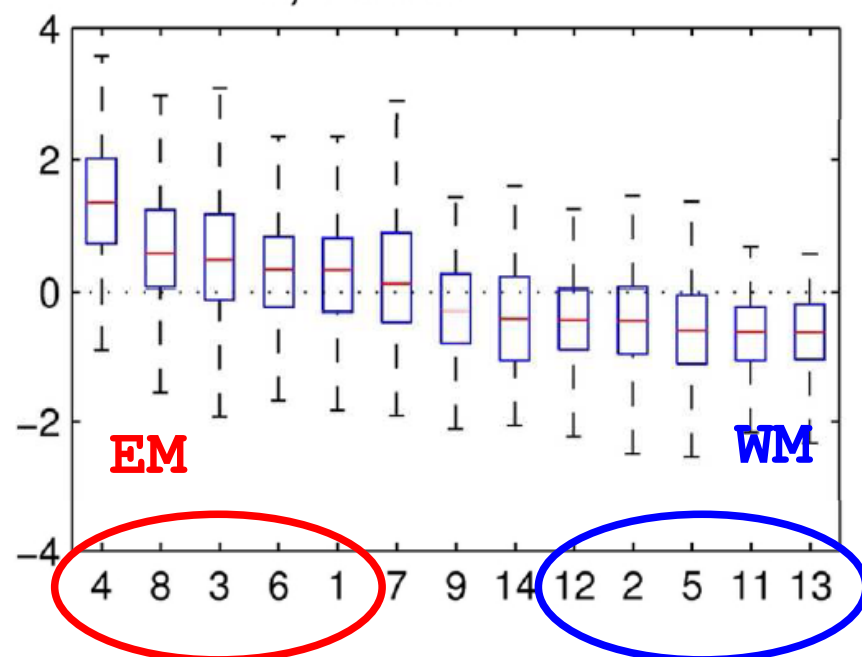
> PXE (s-mode) method with 10 classes to characterize dust/thermal anomalies in the CM (AOD-2 and T850-2).

> PCT (t-mode) method with 14 classes to characterize dust/thermal anomalies in the WM and EM (AOD-1 and T850-1).

c) PCT14 AOD-1

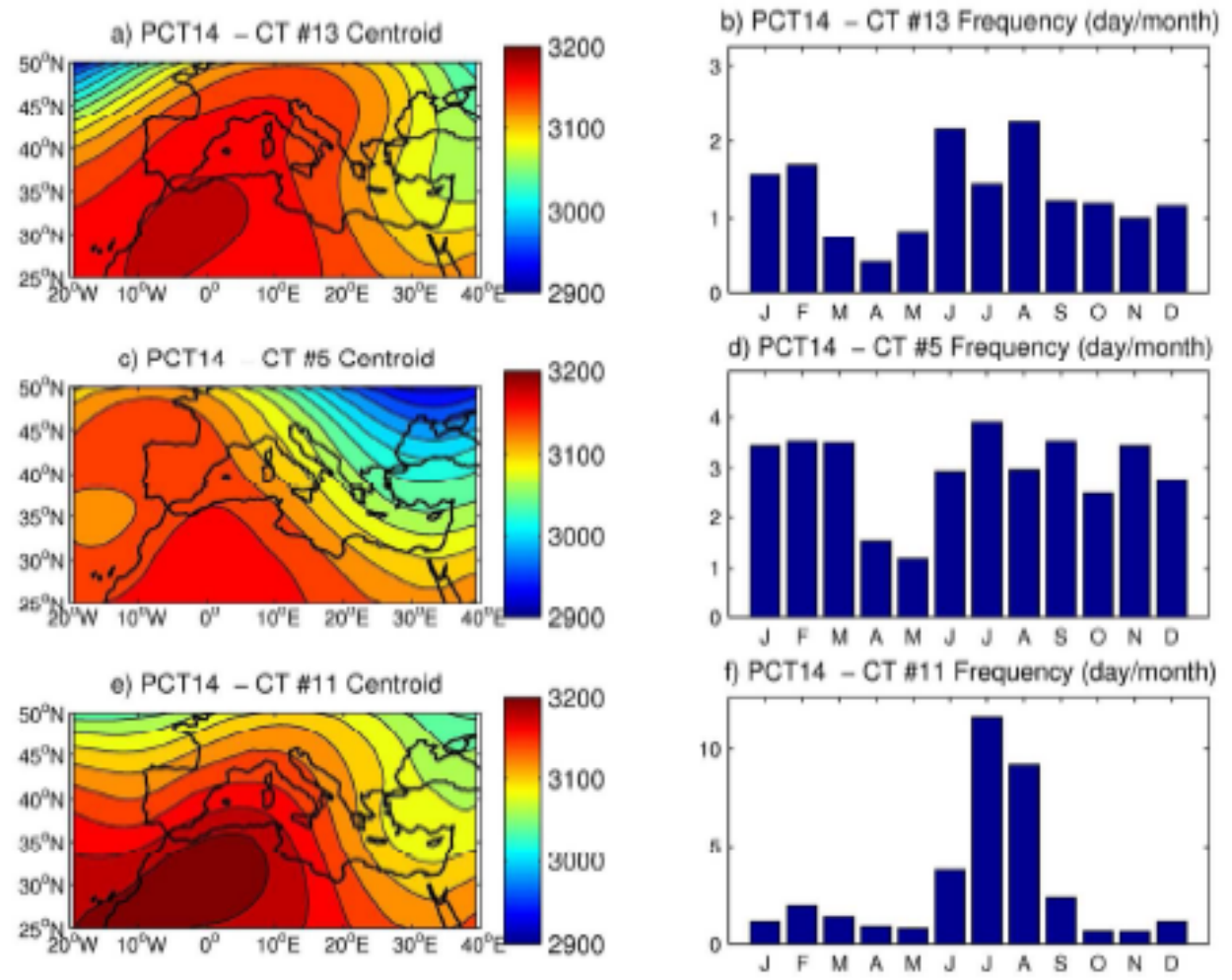


a) PCT14 T850-1



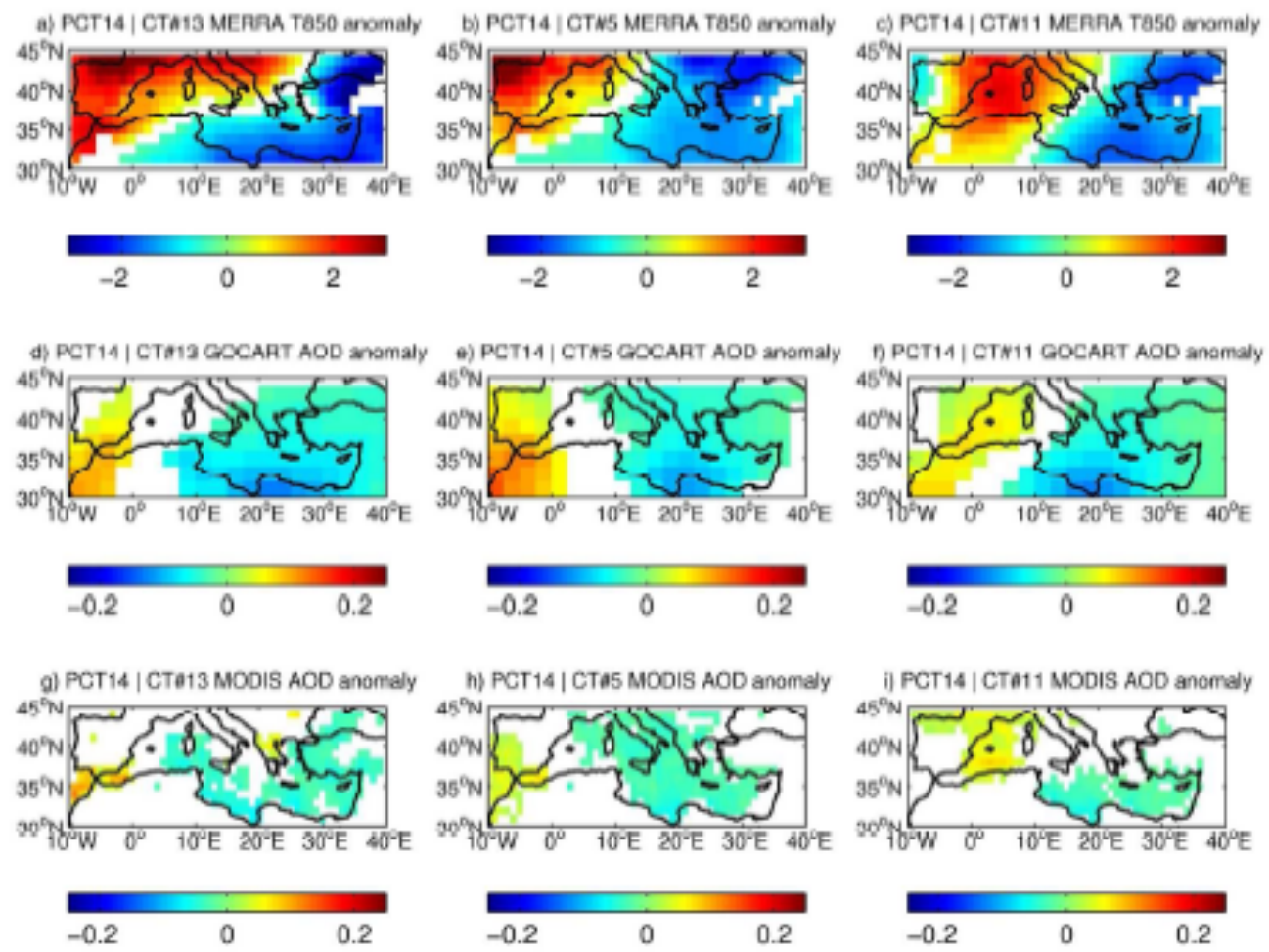
Boxplot of the AOD and T850 indices related to the 1st covariance mode according to the PCT14 circulation patterns: MERRA-GOCART T850-1 and MERRA-GOCART AOD-1. On each box, the central mark is the median, the edges of the box are the 25th and 75th percentiles, the whiskers extend to the most extreme data points not considered outliers. The circulation patterns are sorted according to the median value.

# Selected CTs characterizing WM



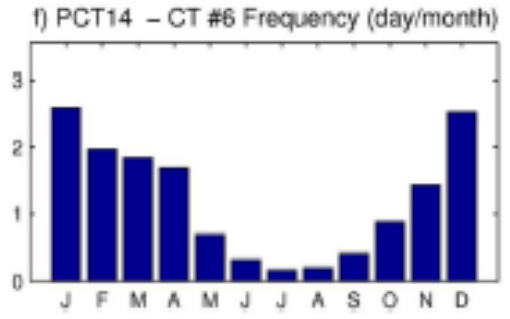
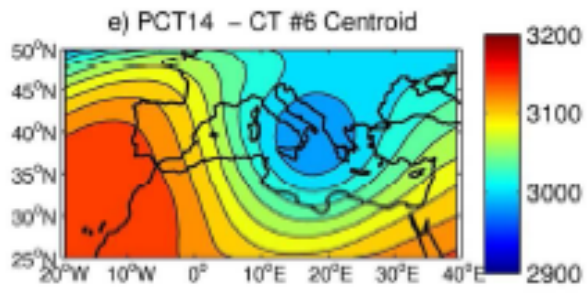
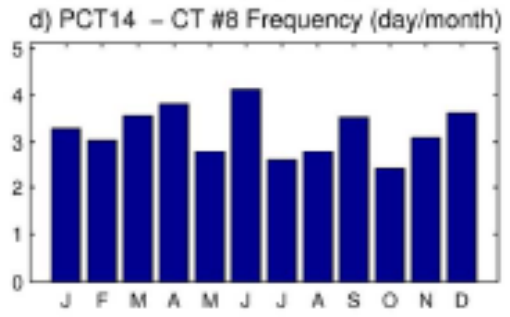
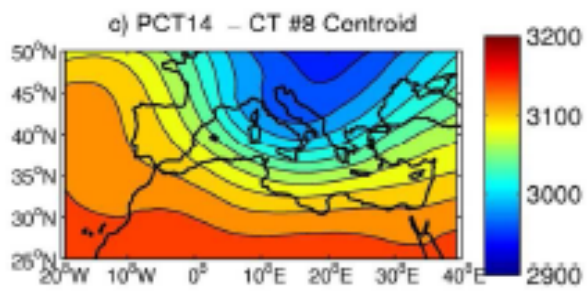
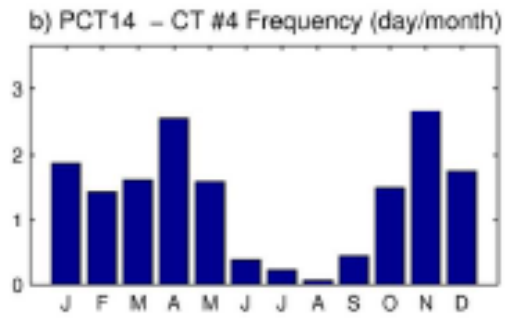
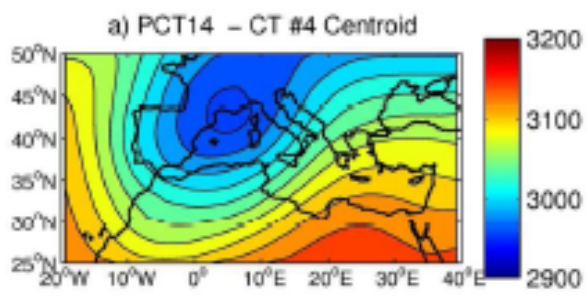
Centroids (left column) and climatological frequencies (right column) of the CT13 (a,b), CT5 (c,d) and CT11 (e,f) derived from the PCT14 classification.

# Composite anomalies: T850, GOCART-AOD, MODIS-AOD

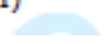


Composites of the daily anomalies associated to the PCT14 CT13 (left column), CT5 (middle column) and CT11 (right column): MERRA T850 (a,b,c), GOCART AOD (d,e,f) and MODIS AOD (g,h,i). Shadings are 99% significant values, after a t-Student test.

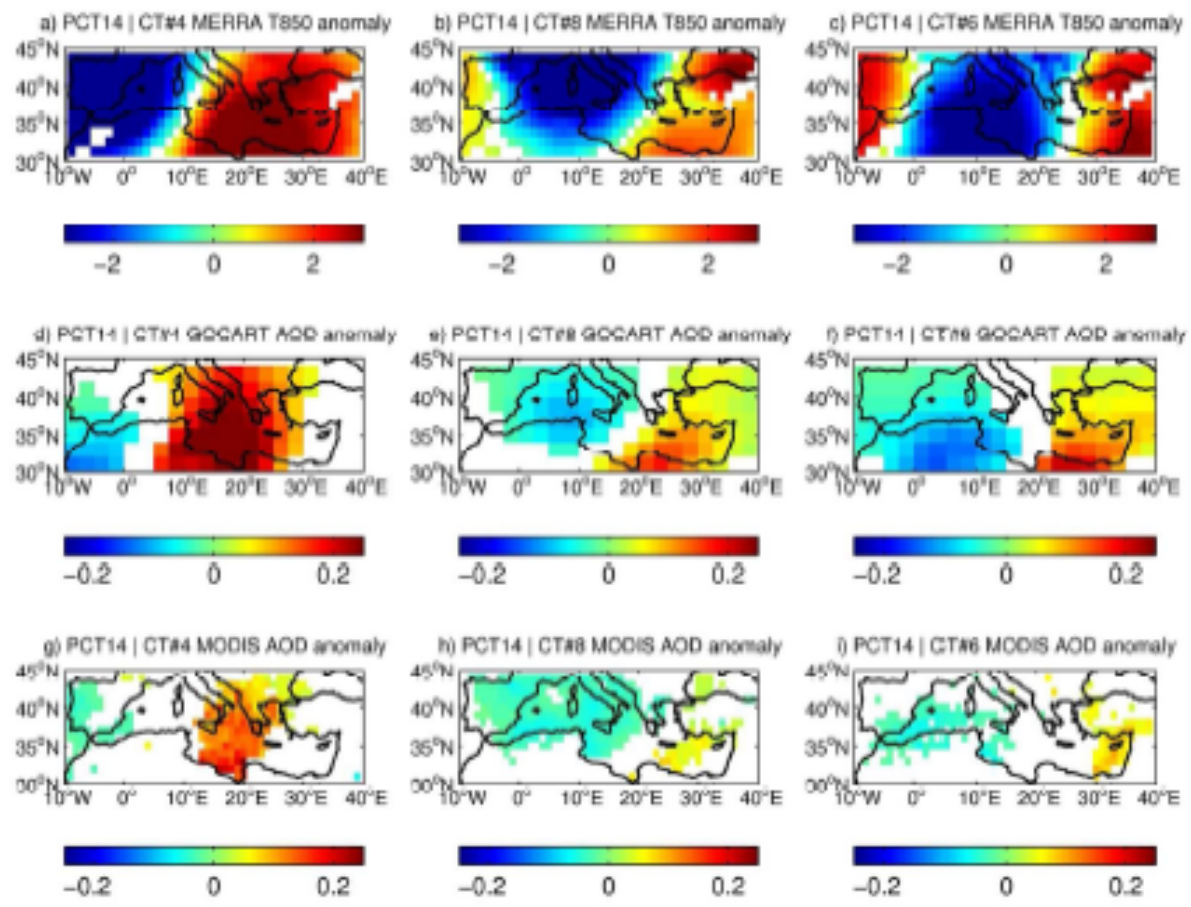
# Selected CTs characterizing EM



Centroids (left column) and climatological frequencies (right column) of the CT4 (a,b), CT8 (c,d) and CT6 (e,f) derived from the PCT14 classification.  
 136x109mm (300 x 300 DPI)



# Composite anomalies: T850, GOCART-AOD, MODIS-AOD



Composites of the daily anomalies associated to the PCT14 CT14 (left column), CT8 (middle column) and CT6 (right column): MERRA T850 (a,b,c), GOCART AOD (d,e,f) and MODIS AOD (g,h,i). Shadings are 99% significant values, after a t-Student test.

130x98mm (300 x 300 DPI)

Gaetani M., M. Pasqui, A. Crisci and F. Guarnieri, 2012. A synoptic characterization of the dust transport and associated thermal anomalies in the Mediterranean basin. *International Journal of Climatology*, doi:JOC-12-0040, under review.

